A Raman spectroscopic study of bukovskýite $Fe_2(AsO_4)(SO_4)(OH)\cdot 7H_2O$-a mineral phase with a significant role in arsenic migration

Jan Loun, [1] Jiří Čejka, [1,2] Jiří Sejkora,[1] Jakub Plášil, [1] Milan Novák, [3]
Ray L. Frost,[2] • Sara J. Palmer [2], Eloise C. Keeffe [2]

[1] National Museum, Václavské náměstí 68, CZ-115 79 Praha 1, Czech Republic.

[2] Chemistry Discipline, Faculty of Science and Technology, Queensland University of Technology, GPO Box 2434, Brisbane Queensland 4001, Australia.

[3] Department of Geological Sciences, Masaryk University, Kotlářská 2, 611 37 Brno, Czech Republic.

ABSTRACT

The Raman spectrum of bukovskýite, $Fe^{3+}_2(OH)(SO_4)(AsO_4)\cdot 7H_2O$ has been studied and compared with the Raman spectrum of an amorphous gel containing specifically Fe, As and S elements and is understood as an intermediate product in the formation of bukovskýite. Observed bands are assigned to the stretching and bending vibrations of $(SO_4)^{2-}$ and $(AsO_4)^{3-}$ units, stretching and bending vibrations and librational modes of hydrogen bonded water molecules, stretching and bending vibrations of hydrogen bonded $(OH)^-$ ions and Fe^{3+}-(O,OH) units. Approximate range of O-H...O hydrogen bond lengths is inferred from the Raman spectra. Raman spectra of crystalline bukovskýite and of the amorphous gel differ in that the bukovskýite spectrum is more complex, observed bands are sharp, the degenerate bands of $(SO_4)^{2-}$ and $(AsO_4)^{3-}$ are split and more intense. Lower wavenumbers of δ H_2O bending vibration in the spectrum of the amorphous gel may indicate the presence of weaker hydrogen bonds compared with those in bukovskýite.

KEYWORDS: bukovskýite, Raman spectroscopy, arsenate, sulfate, hydroxyl ions, molecular water

• Author to whom correspondence should be addressed (r.frost@qut.edu.au)

INTRODUCTION

The mobility of arsenate anions in aqueous media, sediments and wasted soils is of great environmental significance [1-4]. In acid oxidizing surroundings containing Fe^{3+} ions, the question is asked: is the As mobility controlled by the formation of Fe^{3+} sulfoarsenates. bukovskýite $Fe^{3+}_2(AsO_4)(SO_4)(OH)\cdot 7H_2O$ is a member of the relatively small group of naturally Fe^{3+} sulfoarsenates which includes 12 mineral species. Other included minerals in this group are e.g. zýkaite $Fe^{3+}_4(AsO_4)_3(SO_4)(OH)\cdot 15H_2O$, sarmientite $Fe^{3+}_2(AsO_4)(SO_4)(OH)\cdot 5H_2O$, tooeleite $Fe^{3+}_6(AsO_3)_4(SO_4)(OH)_4\cdot 4H_2O$, beudantite $PbFe^{3+}_3(AsO_4)(SO_4)(OH)_6$ and amorphous, not very well defined mineral pitticite $Fe^{3+}_x(AsO_4)_y(SO_4)(OH)_z\cdot 9\ H_2O$ [5].

Bukovskýite was described as a new mineral from the locality Kaňk near Kutná Hora, Czech Republic in 1967 by Novák et al. [6] It occurs there as a (sub)recent weathering product of arsenopyrite and pyrite within the medieval waste dumps. Bukovskyite was collected a long time ago from the pit heaps by the inhabitants of Kutná Hora. It was used for poisoning fieldmice and other field vermin. This poisonous clay, known also by the place name as "toxic clay of Kutná Hora", was widely known in the 19th century.

Pale yellowish-white to grayish-yellow microcrystalline aggregates of bukovskýite forming nodules usually several cm across but locally up to ~1 m in size common occurs in assemblages along with Fe^{3+} arsenates and sulfoarsenates (scorodite, parascorodite, kaňkite, zýkaite) and less common with sulfates (gypsum, melanterite, jarosite, aluminite, alunogen, rozenite). Bukovskýite was later found in distinct environments. Most often it occurs at mine waste dumps [7-11] and mine pit lakes [12,13], naturally it has been identified in As-rich tropical soils [14], in Gard (France) occurs as a component of precipitates of acidic mine waters [15] and it also has been found as a product of oxidation of sulphides by bacteria in the BIOX process [16]. Bukovskýite forms usually at strongly acidic conditions and its stability was calculated on the basis of the ideal mixing model [17]. Mentioned occurrences show that bukovskýite could play a significant role in controlling the migration of arsenic in different environments.

As a part of our on-going research into supergene mineral formation [18,19], this paper reports the Raman spectra of bukovskýite and a similar colloidal mineral phase and relates the spectra to the molecular structure of this sulfoarsenate mineral [20,21]. Infrared spectrum of

bukovskýite in the range from 2000 to 600 cm^{-1} has been published by Novák *et. al.* [6] and in part interpreted. Raman and infrared spectra of bukovskýite were presented in the RRUFF database (R050630), but, as usual, without any interpretation.

EXPERIMENTAL

Minerals

The studied samples were found at medieval mine dumps at Kaňk village, Kutná Hora deposit, central Bohemia, Czech Republic. Two types of macroscopically similar nodules were observed. The first one is represented by pale yellow nodules up to 5 cm in size formed by small (up to 10 μm) lath-like crystals. According to X-ray powder diffraction this type is bukovskýite and no minor significant impurities were found. Its refined unit-cell parameters for the triclinic space group *P*-1, a = 10.770 (1), b = 14.152 (2), c = 10.344 (1) Å, α = 93.14 (1), β = 115.85 (1), γ = 90.20 (1)°, V = 1416.2 (3) $Å^3$, are comparable with the data published for this mineral phase [22]. The second type of nodules with the same size is different in colour - it varies from dark orange to orange-brownish. The X-ray powder diffraction of this type revealed its amorphous character.

Both types of nodules were quantitatively analysed by Cameca SX 100 microprobe system in wavelength dispersion mode for chemical composition. The studied sample was mounted into the epoxide resin and polished. The polished surface was coated with carbon layer 250 Å. An acceleration voltage of 15 kV, a specimen current of 10 nA, a beam diameter of 10 μm and a suite of well-defined natural and synthetic standards were used. The raw intensities were converted to the concentrations using automatic *PAP* matrix correction software package. The H_2O content was calculated from theoretical content of hydroxyls and water molecules.

The chemical composition of the bukovskýite were Fe_2O_3 36.20, As_2O_5 22.01, SO_3 16.13, P_2O_5 0.73, $H_2O_{calc.}$ 30.17 sum 105.23 wt. % and the empirical formula on the basis (Fe+As+S+P) = 4.00 *apfu* is $Fe^{3+}_{2.12}[(AsO_4)_{0.89}(PO_4)_{0.05}]_{\Sigma 0.94}(SO_4)_{0.94}(OH).7H_2O$ (mean of 4 point analyses). There exist only limited As - P isomorphic substitution at the tetrahedral site of bukovskýite. The study of the second type of nodules under high magnification shows that the material is composed mostly of a gel-like medium [23] with a range of chemical

composition (Fe_2O_3 2.95-59.39, As_2O_5 1.49-35.30, SO_3 1.26-7.12, P_2O_5 0.20-4.23, SiO_2 0.20-29.92, Al_2O_3 0.01-7.17, CaO 0.05-4.47 wt. %). Observed gel-like nodules containing Fe, As, S and P may be probably understood as an intermediate in the formation/transformation of bukovskýite nodules [17,23]. In the bukovskýite structure, S ⇔ As substitution may be expected [24,25].

Raman spectroscopy

Microcrystalline aggregates of studied mineral phases were placed on a polished metal surface on the stage of an Olympus BHSM microscope, which is equipped with 10x, 20x, and 50x objectives. The microscope is part of a Renishaw 1000 Raman microscope system, which also includes a monochromator, a filter system and a CCD detector (1024 pixels). The Raman spectra were excited by a Spectra-Physics model 127 He-Ne laser producing highly polarised light at 633 nm and collected at a nominal resolution of 2 cm^{-1} and a precision of ± 1 cm^{-1} in the range between 200 and 4000 cm^{-1}. Repeated acquisition on the crystals using the highest magnification (50x) were accumulated to improve the signal to noise ratio in the spectra. Spectra were calibrated using the 520.5 cm^{-1} line of a silicon wafer. Alignment of all crystals in a similar orientation has been attempted and achieved.

Spectral manipulation such as baseline correction/adjustment and smoothing were performed using the Spectracalc software package GRAMS (Galactic Industries Corporation, NH, USA). Band component analysis was undertaken using the Jandel 'Peakfit' software package that enabled the type of fitting function to be selected and allows specific parameters to be fixed or varied accordingly. Band fitting was done using a Lorentzian-Gaussian cross-product function with the minimum number of component bands used for the fitting process. The Gaussian-Lorentzian ratio was maintained at values greater than 0.7 and fitting was undertaken until reproducible results were obtained with squared correlations of r^2 greater than 0.995.

RESULTS AND DISCUSSION

The Raman spectra of both studied nodules are shown in Figs. 1a and 1b (1700-700 cm^{-1}), 2a and 2b (700-100 cm^{-1}), and 3a and 3b (3800-2600 cm^{-1}), respectively. The presence of $(SO_4)^{2-}$, $(AsO_4)^{3-}$, $(OH)^-$ ions and water molecules are inferred from the Raman spectra

(Table 1). The T_d symmetry is characteristic for both free units $(SO_4)^{2-}$ and $(AsO_4)^{3-}$. In dilute aqueous solutions $(SO_4)^{2-}$ ions exhibit the symmetric stretching vibration (A_1, ν_1), 983 cm^{-1} – Raman active, the doubly degenerate bending vibration (E, ν_2), 450 cm^{-1} – Raman active, the triply degenerate antisymmetric stretching vibration (F_2, ν_3), 1105 cm^{-1} – Raman and infrared active, and the triply degenerate bending vibration (F_2, ν_4), 611 cm^{-1} – Raman and infrared active. Any symmetry lowering may activate some or all vibrations in both Raman and IR and cause the splitting of degenerate vibrations [26-28]. Fundamental vibrational modes for $(AsO_4)^{3-}$ are the symmetric stretching vibration (A_1, ν_1), 837 cm^{-1} – Raman active, the doubly degenerate bending vibration (E, ν_2), 349 cm^{-1} – Raman active, the triply degenerate antisymemtric stretching vibration (F_2, ν_3) – 878 cm^{-1} – Raman and infrared active, and the triply degenerate bending vibration (F_2, ν_4), 463 cm^{-1} – Raman and infrared active. Similarly as in the case of sulfate ions any symmetry lowering may cause Raman and infrared activation of some or all vibrations and the splitting of degenerate vibrations [26, 29]. Observed Raman spectra of bukovskýite (A) are compared with those of gel-like nodules of variable composition containing mostly amorphous Fe^{3+} arsenate, Fe^{3+} sulfoarsenate and gel of $SiO_2 \cdot xH_2O$ (B).

Bands at 1179, 1131, ~1090, 1054 and ~1010 cm^{-1} (A) and 1122 and 1050 cm^{-1} (B) are assigned to the split ν_3 $(SO_4)^{2-}$ antisymmetric stretching vibrations (Fig. 1). However, some of these bands may be connected with the δ Fe-OH deformation modes. Bands at 984 cm^{-1} (A) and 993 cm^{-1} (B) are attributed to the ν_1 $(SO_4)^{2-}$ symmetric stretching vibrations. Bands at 886, 847 and 816 cm^{-1} (A) and 873 and 814 cm^{-1} (B) are attributed to the $(AsO_4)^{3-}$ ν_3 antisymmetric and ν_1 symmetric stretching vibrations, while the band at 911 cm^{-1} (A) may be assigned to the ν_3 $(AsO_4)^{3-}$ or δ Fe-OH or libration of water molecules. In this region (1200-700 cm^{-1}), the Raman spectrum of bukovskýite (A) exhibits more bands than that of the amorphous gel (B) and their higher intensity and sharpness. This may be caused by the crystallinity of bukovskýite (A) in comparison with the amorphous gel (B) and the splitting of the degenerate vibrations because of T_d symmetry lowering of $(SO_4)^{2-}$ and $(AsO_4)^{3-}$ tetrahedra. Band intensities observed in the Raman spectrum of the amorphous gel (B) is substantially lower than those in the Raman spectrum of bukovskýite (A).

Bands at 613, 552 and 511 cm^{-1} (A) and 496 cm^{-1} (B) are assigned to the ν_4 $(SO_4)^{2-}$ bending vibrations and those at 464 and 428 cm^{-1} (A) and 445 cm^{-1} (B) to the ν_2 $(SO_4)^{2-}$

bending vibrations, the ν_4 $(AsO_4)^{3-}$ bending vibrations, and Fe-O and Fe-OH stretching vibrations (Fig. 2). A band at 315 cm^{-1} (A) may be attributed to the ν_2 $(AsO_4)^{3-}$ or Fe-O or Fe-OH stretching vibrations [30]. Bands at 263 cm^{-1} (A) and 244 cm^{-1} (B) are connected with the ν OH...O stretching vibrations [31] . Bands at 196 and 147 cm^{-1} (A) and 180 and 145 cm^{-1} are assigned to the lattice vibrations. In this region (700-100 cm^{-1}), Raman spectrum of bukovskýite (A) also differs from that of the amorphous gel in the number of observed bands and their intensities. The reason for it is that the T_d symmetry lowering of $(SO_4)^{2-}$ and $(AsO_4)^{3-}$ tetrahedra may cause the splitting of the degenerate vibrations in the Raman spectrum of crystalline bukovskýite (A) when compared with the Raman spectrum of the amorphous gel (B).

Bands at 3420, 3219 and 3102 cm^{-1} (A) and 3421, 3220 and 2940 cm^{-1} (B) are assigned to the ν OH stretching vibrations of hydrogen bonded hydroxyls and hydrogen bonded water molecules (Fig. 3). O-H...O hydrogen bond lengths calculated from positions of these vibrations according Libowitzky [32] equation vary in the range 2.82-2.68 Å (A) and 2.82-2.65 Å (B). Bands at 1652 cm^{-1} (A) and 1625 cm^{-1} (B) are attributed to the δ H_2O bending vibrations. The lower wavenumber (B) may indicate the presence of weaker hydrogen bonds in the amorphous gel than in crystalline bukovskýite.

The role of bukovskýite at the mechanism of arsenic migration and entrapment

The nodules studied primarily by EMPA revealed the crystallization of bukovskýite needle-like crystals from Fe,As,S-bearing Si-Al gel-like medium. Two different types of this medium were distinguish: „dark“ type (dark in BSE images) enriched in Si and Al and „light“ type enriched in Fe and As. The gel-like medium is a product of dissolution of various minerals of the dump at strongly acidic conditions (pH = 2.4-3.9). The chemical composition of gel-like medium is related to the theoretical composition of bukovskýite. Bukovskýite finally crystallized from light „gels“ which are closer to the bukovskýite stoichiometry and dark type remains usually as a relict in residual space [23]. The origin of relatively stable bukovskýite from Si-Al rich gel-like medium in clayey parts of tips and similar media thus represents the possibility of As capture in solid-solution phase and makes a barrier for free migration of this element into surroundings.

CONCLUSIONS

(1) Macroscopically similar aggregates of bukovskýite and an amorphous Fe-As-S-Si gel phase from the same locality (Kaňk near Kutná Hora, Czech Republic) have been studied.

(2) The formation of the bukovskýite mineral presents a mechanism for arsenate absorption and removal from the environment

(3) Both types of nodules can be easily distinguished with Raman spectroscopy; differences between both studied samples may be inferred especially with the intensities of the Raman bands attributed to sulphate ions. The more distinctive character of crystalline bukovskýite is readily recognised by its Raman spectrum.

(4) Observed Raman bands were tentatively assigned to the stretching and bending vibrations of $(SO_4)^{2-}$, $(AsO_4)^{3-}$ and hydrogen bonded $(OH)^-$ ions, to the stretching and bending vibrations and libration modes of hydrogen bonded water molecules, to Fe-(O,OH) stretching vibrations and to lattice vibrations.

(5) Approximate range of O-H...O hydrogen bond lengths (bukovskýite, 2.82-2.68 Å; amorphous gel phase, 2.82-2.65 Å) were inferred from the Raman spectra.

Acknowledgements

The financial and infra-structure support of the Queensland University of Technology Chemistry Discipline is gratefully acknowledged. The Australian Research Council (ARC) is thanked for funding the instrumentation. This work was financially supported by Ministry of Culture of the Czech Republic (MK00002327201) to Jan Loun, Jiří Sejkora and Jakub Plášil.

232 **Table 1. Interpretation of the Raman spectra of bukovskýite and amorphous Fe-As-S-Si**
233 **gel phase (band position in cm^{-1})**
234
235

bukovskýite	**Fe-As-S-Si gel phase**	**assignment**
3420, 3219, 3102	3421, 3220, 2940	ν OH stretching vibration of H_2O and $(OH)^-$ ions
1652	1625	δ H_2O vibrations
1179, 1131, 1090, 1054, 1010	1122, 1050	ν_3 $(SO_4)^{2-}$ antisymmetric stretch (δ-Fe-OH bend)
984	993	ν_1 $(SO_4)^{2-}$ symmetric stretch
911		ν_3 $(AsO_4)^{3-}$ antisymmetric stretch or Fe-OH bend or libration of water molecules
886, 847, 816	873, 814	ν_3 and ν_1 $(AsO_4)^{3-}$ antisymmetric and symmetric stretch
613, 552, 511	496	ν_4 $(SO_4)^{2-}$ bend
464, 428	445	ν_2 $(SO_4)^{2-}$ bend or ν_4 $(AsO_4)^{3-}$ bend or Fe-O and Fe-OH stretch
315		ν_2 $(AsO_4)^{3-}$ bend or Fe-O or Fe-OH stretch
263	244	ν OH...O stretch
196, 147	180, 145	lattice vibrations

236
237

References

[1] J. G. Hering, P. E. Kneebone, Biogeochemical controls on arsenic occurrence and mobility in water supplies. Chapter *7* in *Environmental Chemistry of Arsenic* (W.T. Frankenberger Jr., Ed.) p. 155-181. Marcel Dekker Inc., New York **2002**.

[2] M. R. Gunsinger, C. J. Ptacek, D. W. Blowes, J. L. Jambor, M. C. Moncur, *Appl. Geochem.* **2006,** *21,* 1301-1321.

[3] A. R. Keimowitz, Y. Zheng, S. N. Chillrud, B. Mailloux, H. B. Jung, M. Stute, H. J. Simpson, *Environ. Sci. Technol.* **2005,** *39,* 8606-8613.

[4] R. L. Frost, S. Bahfenne, J. Čejka, J. Sejkora, J. Plášil, S. J. Palmer, *J. Raman Spectrosc*. (in print), DOI: 10.1002/jrs2356.

[5] J. W. Anthony, R. A. Bideaux, K. W. Bladh, M. C. Nichols, Handbook of Mineralogy. Volume IV, Arsenates, Phosphates, Vanadates. 680 pp., Mineral Data Publishing, Tucson Arizona **2000**.

[6] F. Novák, P. Povondra, J. Vtělenský, *Acta Univ. Carol., Geol.,* **1967**, 4, 297-325.

[7] T. Witzke, M. Hocker, *Lapis* **1993**, *18***,** 49.

[8] J. Hyršl, M. Kaden, *Aufschluss* **1992**, *43*, 95.

[9] W. H. Paar, J. Weidinger, R. Mrazek, H. Heiss, *Lapis* **1993**, *18*, 13.

[10] U. Baumgärtl, J. Burow, *Aufschluss* **2002**, *53*, 278.

[11] D. Mains, D. Craw, *J. Geol. Geophys.*, **2005**, *48*, 641.

[12] R. J. Bowell, J. V. Parshley, *Chem. Geol.*, **2005**, *215*, 373.

[13] S. Triantafyllidis, N. Skarpelis, *J. Geochem. Explor.*, **2006**, *88*, 68.

[14] R. J. Bowell, *Mineral. Mag.*, **1992**, *56*, 545.

[15] M. Leblanc, B. Achard, D. B. Othman, J. M. Luck, *Appl. Geochem.*, **1996**, *11*, 541

[16] M. Márquez, J. Gaspar, K. E. Bessler, G. Magela, *Hydrometallurgy*, **2006**, *83*, 114.

[17] O. L. Gas'kova, G. P. Shironosova, S. B. Bortnikova, *Geochem. Internat.*, **2008**, *46*, 92-99.

[18] J. Sejkora, J. Škovíra, J. Čejka, J. Plášil, *J. Geosci*. **2009**, *54***,** 355-371.

[19] J. Sejkora, D. Ozdín, R. Ďuďa, *J. Geosci*. **2010**, *55***,** 149-160.

[20] R. L. Frost, S. Bahfenne, J. Čejka, J. Sejkora, J. Plášil, S. J. Palmer, *J. Raman Spectrosc*. **2010**, *41***,** 814-819.

[21] R. L. Frost, S. Bahfenne, J. Čejka, J. Sejkora, S. J. Palmer, R. Škoda, *J. Raman Spectrosc.* **2010**, *41***,** 690-693

[22] Z. Johan, *Neues Jb. Mineral. Mh*. **1986**, *10*, 445-451.

[23] J. Loun, *MS, graduation theses, PřF MU, Brno*. **2010**.

[24] D. Paktunc, J.E. Dutrizac, *Can. Mineral.* **2003,** *41*, 905-919.

[25] D. Paktunc, Proceedings of the 24th IAGS, Fredericton **2009,** 881-884.

[26] K. Nakamoto, *Infrared and Raman Spectra of Inorganic and Coordination Compounds*, Wiley and Sons, New York, **1986**.

[27] S.C.B. Myneni, *Rev. Mineral.* **2000**, *40*, 113-172.

[28] M.D. Lane, *Am. Mineral.* **2007**, *92*, 1-18.

[29] P. Keller, *Neues Jb. Mineral. Mh.* **1971** H. 11, 491-510.

[30] H.D. Lutz, *Struct. Bonding* **1995**, *82, 85-103.*

[31] F.K. Vansant, B.J. Van Der Veken, H.O. Desseyn, *J. Mol. Struct.* **1973**, *15*, 425-437.

[32] E. Libowitzky, *Monatsh. Chem.* **1999**, *130*, 1047-1059.

List of Table

Table 1. Interpretation of the Raman spectra of bukovskýite and amorphous Fe-As-S-Si gel phase (band position in cm^{-1})

List of Figures

Fig. 1a Raman spectrum of bukovskýite in the 1700 to 700 cm^{-1} region.

Fig. 1b. Raman spectrum of amorphous Fe-As-S-Si gel phase in the 1700 to 700 cm^{-1} region.

Fig. 2a Raman spectrum of bukovskýite in the 700 to 100 cm^{-1} region.

Fig. 2b Raman spectrum of amorphous Fe-As-S-Si gel phase in the 700 to 100 cm^{-1} region.

Fig. 3a Raman spectrum of bukovskýite in the 3800 to 2600 cm^{-1} region.

Fig. 3b Raman spectrum of amorphous Fe-As-S-Si gel phase in the 3800 to 2600 cm^{-1} region.

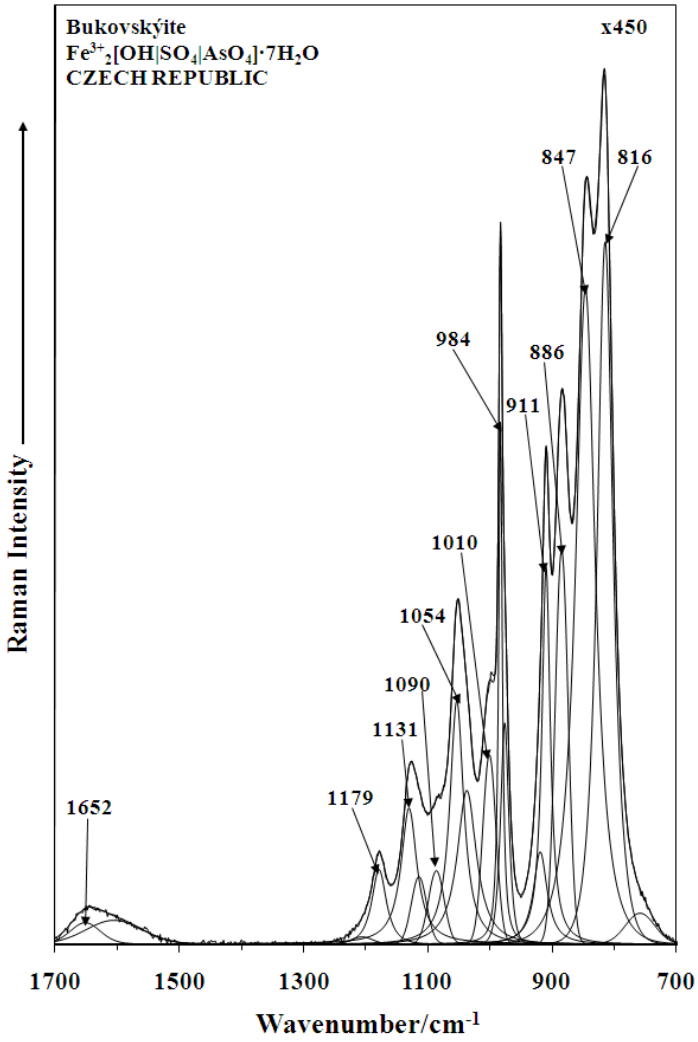

Fig. 1a Raman spectrum of bukovskýite in the 1700 to 700 cm^{-1} region.

316

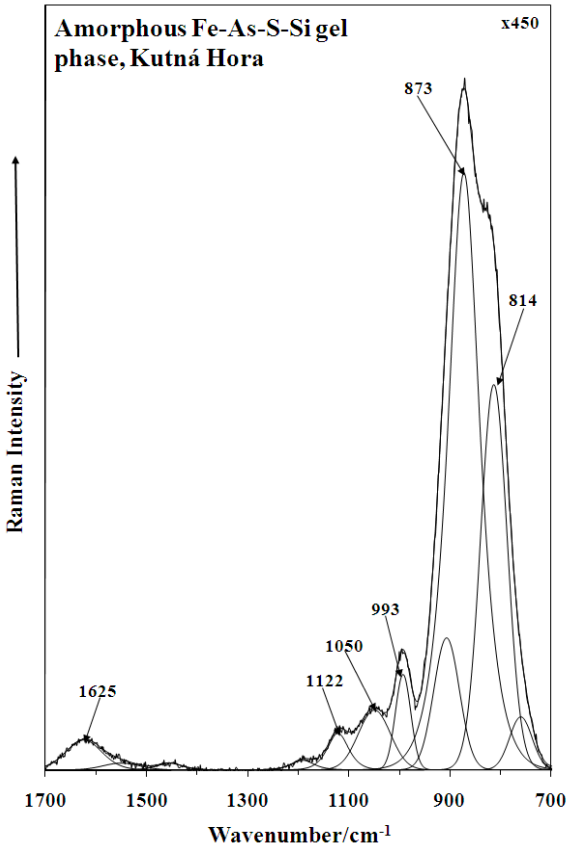

317

318

319

320 **Fig. 1b. Raman spectrum of amorphous Fe-As-S-Si gel phase in the 1700 to 700 cm^{-1}**

321 **region.**

322

323

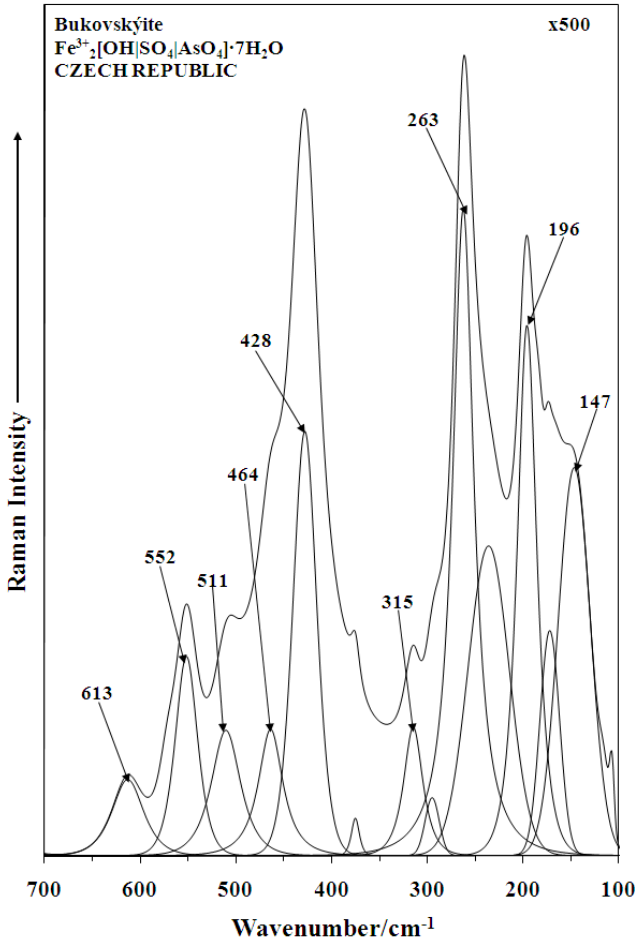

Fig. 2a Raman spectrum of bukovskýite in the 700 to 100 cm^{-1} region.

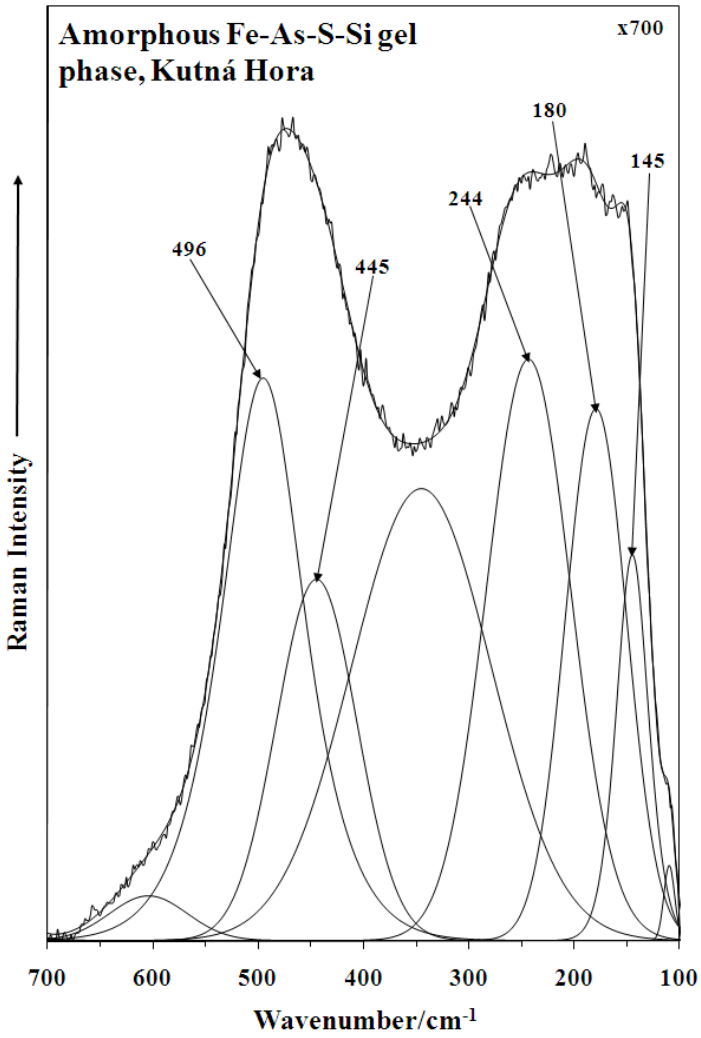

328

329

330 **Fig. 2b Raman spectrum of amorphous Fe-As-S-Si gel phase in the 700 to 100 cm^{-1}**

331 **region.**

332

333

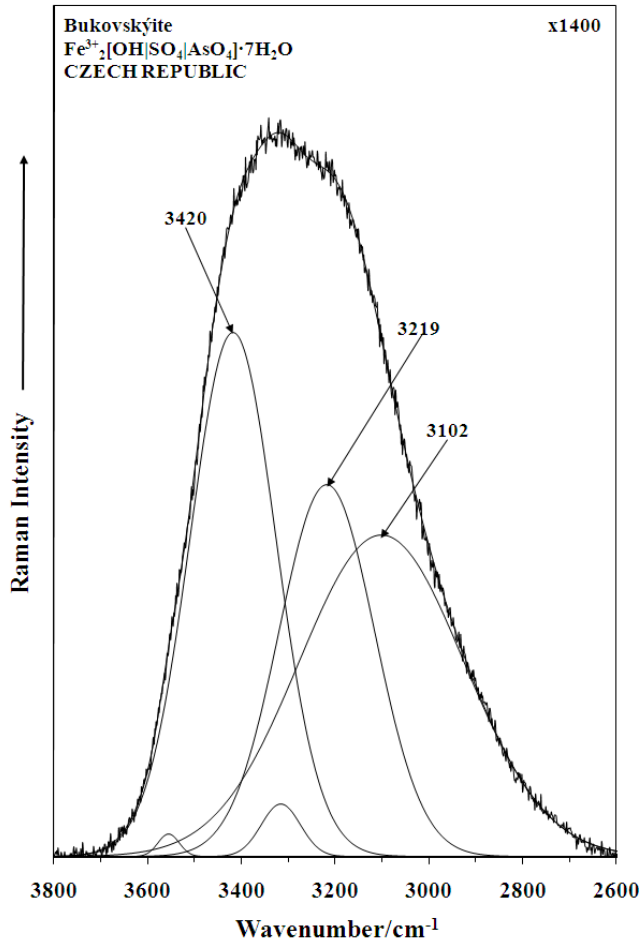

Fig. 3a Raman spectrum of bukovskýite in the 3800 to 2600 cm^{-1} region.

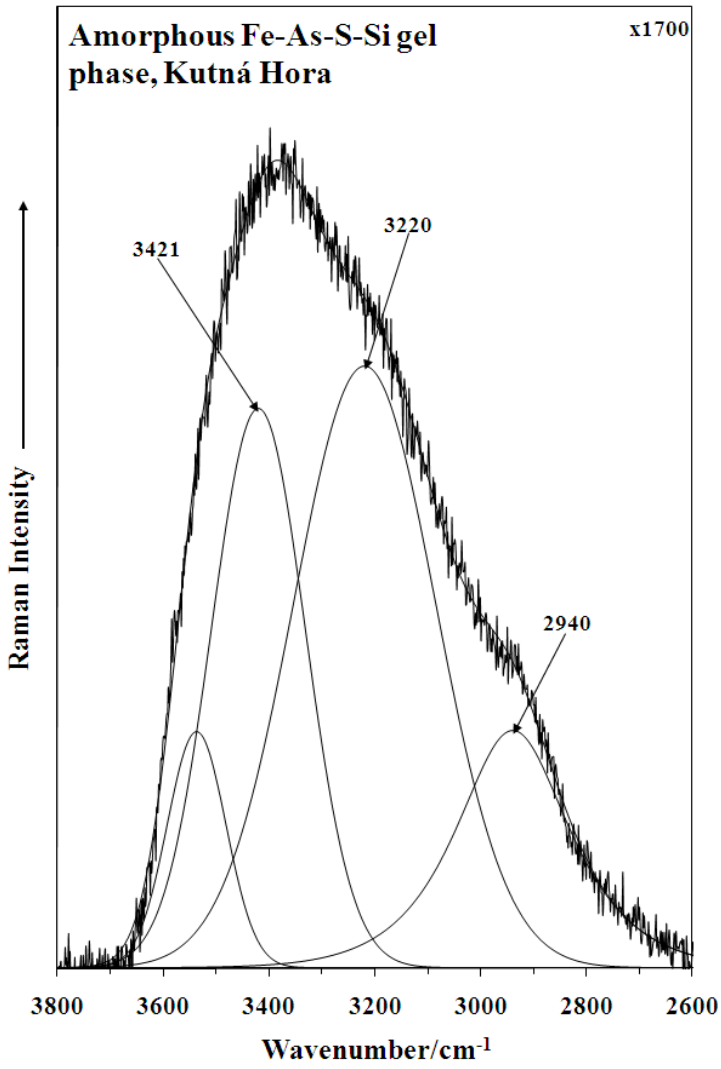

342

343

344 **Fig. 3b Raman spectrum of amorphous Fe-As-S-Si gel phase in the 3800 to 2600 cm^{-1}**

345 **region.**

346